# Joint Centre for Mesoscale Meteorology, Reading, UK

## Modelling Low Level Winds with the Met Office New Dynamics Model

Rachel Anne Capon

Internal Report No. 133
NWP Scientific Paper No. 66

9 May 2002

**Met Office** Joint Centre for Mesoscale Meteorology Department of Meteorology
University of Reading PO Box 243 Reading RG6 6BB United Kingdom
Tel: +44 (0)118 931 8425 Fax: +44 (0)118 931 8791
www.metoffice.com

*Designed and produced by the Met Office © Crown copyright 2001 01/0240 The Met Office logo is a registered trademark.*

# Modelling Low Level Winds with the Met Office New Dynamics Model

Rachel Anne Capon

*Met Office Joint Centre for Mesoscale Meteorology*

*Meteorology Building University of Reading P.O. Box 243 Reading RG6 6BB*

9 May 2002

## Abstract

It is part of British sailing and forecasting folklore that the wind speed increases in the Dover Straits when there is an established wind-flow — westerly/south-westerly or easterly/north-easterly — along the English Channel. However the underlying mechanism of the phenomenon is unclear.

We have used the New Dynamics mesoscale model to perform a case study on an occasion when this phenomenon was observed in the Channel but not forecast by the operational model. Results are presented showing the sensitivity of forecasts to horizontal resolution (down to 2 km) and to vertical resolution. We also demonstrate the impact of changing the surrounding orography and the land or sea surface roughness.

This work was undertaken under the auspices of the Met Office Low Level Atmospheric Structure Project, the overall long-term objective of which is to establish and to improve the quality of detailed low level atmospheric predictions, especially in the neighbourhood of hills and coasts and with a particular focus on wind speed and direction. We therefore conclude with a discussion of how a very high resolution New Dynamics mesoscale model might be implemented operationally and directions for future work.

# 1 Introduction

## 1.1 Motivation and Aims

It is part of British sailing and forecasting folklore that the wind speed increases in the Dover Straits when there is an established wind-flow along the English Channel. The phenomenon may in fact be most pronounced in an easterly or north-easterly wind, as such winds are usually associated with a synoptic scale anticyclonic pattern over the UK and the corresponding high stability at low levels in the atmosphere.

The Dover Straits are just over 30 km wide at their narrowest point. Hence, they are on the borderline of being resolved by current operational forecast models. It therefore seems unlikely that the wind speed-up phenomenon is correctly captured in current forecasts. Moreover, the underlying physical mechanism of the phenomenon is poorly understood. There are several possible candidates for the mechanism, for example channelling through the orography or the effect of the land-sea surface roughness contrast, both of which we discuss in the following section. However, in the Dover Straits region, the expected scale of these effects appears to be small relative to the wind speed-up observed.

We have used a case study approach to investigate the wind speed-up phenomenon. The work presented here was undertaken under the auspices of the Met Office Low Level Atmospheric Structure Project. Several Met Office teams are working on this Met Support Group funded project. The overall long-term objective is to establish and to improve the quality of detailed low level atmospheric predictions, especially in the neighbourhood of hills and coasts and with a particular focus on wind speed and direction. The specific aim of our work is to investigate and demonstrate the forecasting capability of the Met Office New Dynamics model mesoscale version at high resolution (up to ca. 2 km grid spacing). The New Dynamics model [1], which will become operational during 2002, has several novel features. In particular, it is non-hydrostatic and is therefore able to handle the orography at these scales and to describe the resultant gravity waves correctly. Also, the numerical formulation is semi-Lagrangian, rather than Eulerian. Hence the model can be run with little or no diffusion. Section 2 describes how we tested the sensitivity of the model forecast to both horizontal and vertical resolution and the results obtained.

After thus demonstrating the impact of resolution on the forecast, we also performed a series of numerical experiments, for the same case, in order to investigate the physical mechanism. The values of two physical parameters, the surface roughness length — over land and over the sea — and the height of the orography, were altered in order to assess their relative impacts on the low level wind speed. The results of these experiments are presented in Section 3.

## 1.2 Contributing Factors - Physical Mechanism

There are several factors known to cause acceleration of the wind in a channel. We want to consider which of these may contribute to this phenomenon in the Dover Straits case.

Firstly, we consider the orography. The Dover Straits are 30 - 40 km wide and lie in a gap in the orographic barrier - which is 150 - 200 m high and over 300 km long - formed by the North Downs (on the English side) and the Colline de l'Artois (on the French side). This orography can be seen later in figure 12. Baines [2, 3] performed a series of laboratory experiments on flow past a barrier ridge with a gap. He found that a layer of fluid incident below a certain height would be channelled through the gap if the Froude

number,

$$F = \frac{U}{Nh} < 0.5, \tag{1}$$

where $h$ is the orographic barrier height, $N$ is the buoyancy frequency and $U$ is the wind speed. This result may be applied to the Dover Straits. We know that $h \approx 200m$ and take as a typical atmospheric value, $N \sim 0.01$. From equation (1), we have

$$U < 1ms^{-1} \tag{2}$$

Clearly, either a much higher stability ($N$) and/or a very low wind speed ($U$) are required in the lower atmosphere for the low level flow to be deflected through the gap rather than simply pass over the orography. Alternatively, if there was a very low temperature inversion intersecting the orography, the low level airflow may be forced through the gap. In practice, strong orographic channelling of the wind seems unlikely in most situations in the Dover Straits.

Another possible contributing factor is the roughness length. As the air moves from the sea over the land, the increase in magnitude of the roughness length will cause deceleration of the wind speed and convergence at lower levels. An internal boundary layer will develop. Conversely, air which later moves back over the sea will accelerate and subside.

We should also consider sea and land breezes and drainage flows. A sea breeze may be set up during the day in summer anticyclonic conditions. At surface level, the sea breezes flow in opposing directions towards the English and French coasts. Hence one would expect divergence over the Channel. However, the upper level return flows, which are typically at height $\sim 10^2 - 10^3$ m and also part of the sea-breeze circulation, will converge into the Channel. Furthermore, during the course of the day, an established sea breeze circulation will turn clockwise due to the Coriolis effect. Thus it may act to reinforce along-Channel winds, either at the surface or at higher levels, but this effect will be reversed on the other side of the Channel.

A land breeze may occur during Autumn and Winter in anticyclonic conditions (when the land temperature is low relative to the sea surface temperature) and also at night in summer anticyclonic conditions. Furthermore, it may be reinforced by the katabatic drainage flow of cold air from higher to lower levels. There will be convergence over the Channel and, perhaps, increased wind speed. Turning of the land breeze may also occur.

Although all the above effects can cause wind acceleration, it is not evident that any of them could be of sufficient magnitude to cause the increase in wind speed observed in the Dover Straits region of the English Channel.

## 1.3 23 July 2000 Observations

The specific case of the Dover Straits wind speed-up phenomenon considered in this report occurred on 23 July 2000. This case was brought to our attention by Eddy Carroll, chief forecaster at NMC, Bracknell. The analysis from 0Z on 23 July 2000 and the corresponding radiosonde ascent at Herstmonceux on the south coast of England are shown in figures 1 and 2 respectively. There are north-easterly winds entering the Channel from the North Sea beneath an anticyclonic subsidence inversion. The standard surface observations demonstrate speed-up of the wind in the English Channel. Additional observations from the Hoverspeed craft operating between Dover and Calais, provided by Julian Hunt, correlate well with the observed winds and show the speed-up starting at the entrance to the Dover Straits.

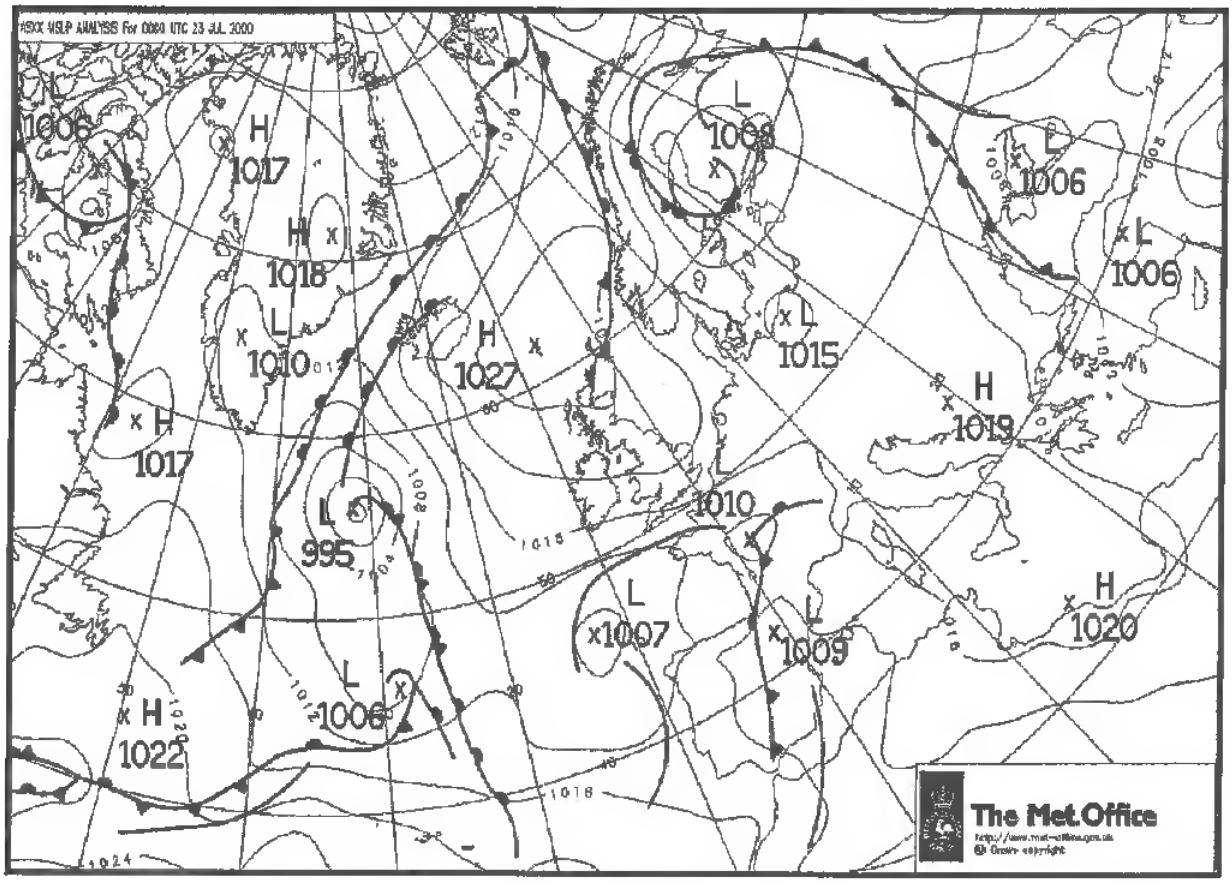


Figure 1: Analysis at 0Z 23/07/00. Note the anticyclone centred north of Scotland and affecting the whole of the UK.

Figure 3 shows the observations from 9Z on 23/07/2000 in the English Channel. These show a wind speed of 20 knots, as the wind enters the Dover Straits at their eastern end, at Sandettie (51°9' N, 1°47' E). Similar wind speeds were reported by the first Hovercraft voyages between 07Z and 09Z. Further downstream, Greenwich light vessel (on the Meridian at 50°25' N, 0°E) reported winds of up to 30 knots for most of the day. Notably, the 30 knot winds reported at Greenwich light vessel were super-geostrophic — the geostrophic wind being ca. 20-25 knots — and considerably stronger than predicted by the operational ("Old Dynamics") model forecast.

# 2 New Dynamics Model Forecasts: Resolution Tests

## 2.1 Method

We modelled this case by running the New Dynamics (ND) v3.0 mesoscale model for 24 hours from 0Z on 23/07/2000, on three nested limited area domains. Initially we ran the global ND model to produce lateral boundary conditions for the operational mesoscale domain. We then ran the ND mesoscale model on the operational domain - shown in figure 4 - which has a horizontal resolution of 12km. This run will be referred to as 12kL38 in the following discussion. Further runs were carried out at horizontal grid resolutions of 4km (run 4kL38) and 2km (run 2kL38), also shown in figure 4. In each of these cases, New Dynamics vertical level set A, which has 38 model levels in the vertical, designed to

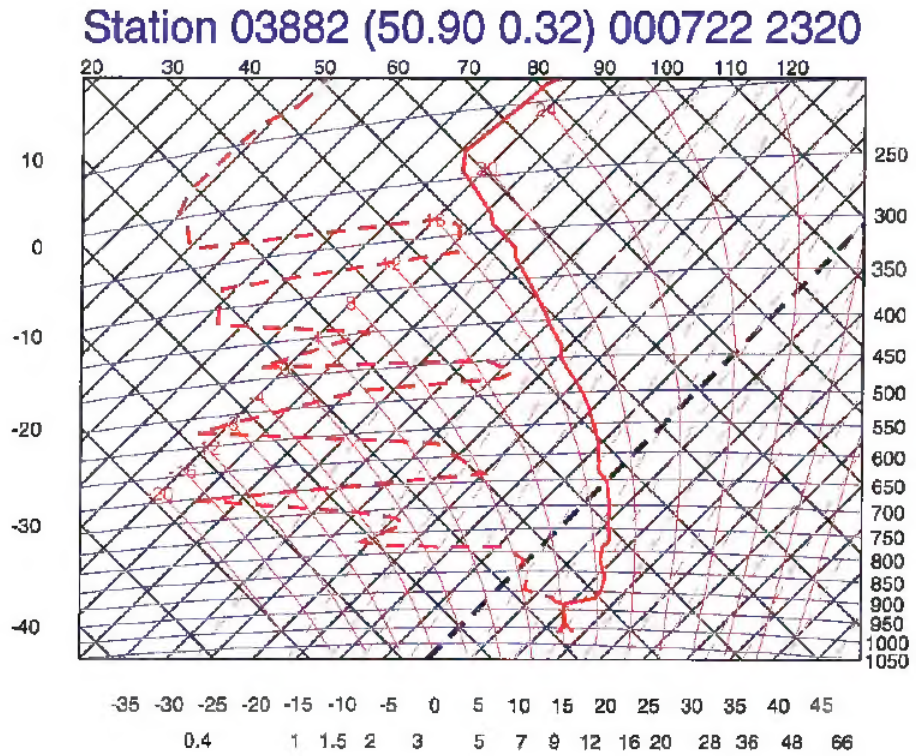


Figure 2: Radiosonde ascent from Herstmonceux, Sussex, at 2320Z 22/07/00, showing a strong temperature inversion at ca. 925mB height.

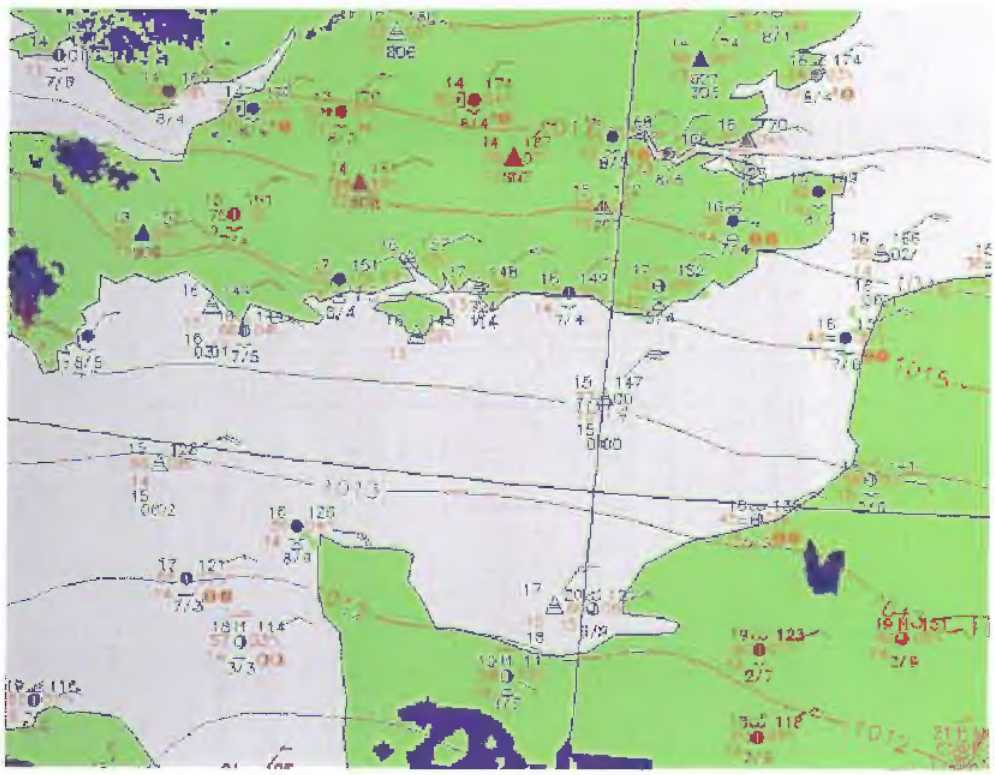

Figure 3: Observations at 09Z 23/07/00. In the English Channel, Greenwich Light Vessel (situated on the Meridian at 50°25' N, 0°E) reported 30 knot winds.

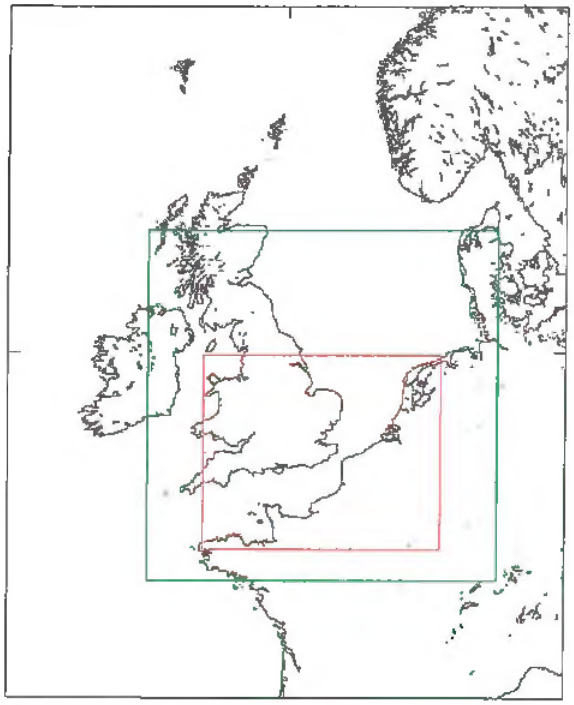

Figure 4: Operation mesoscale domain, showing nested domains with 4km grid and 2km grid respectively.

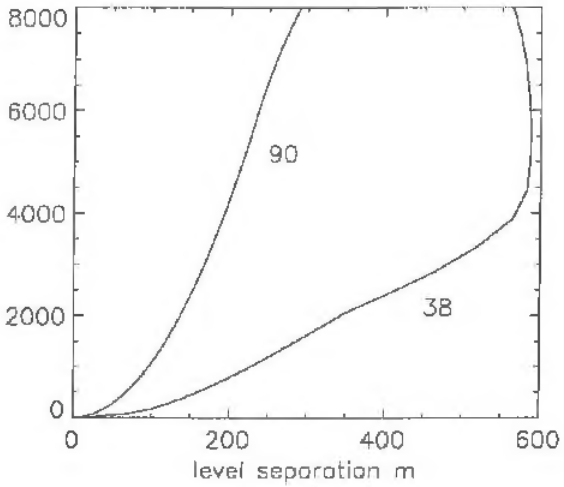


Figure 5: Height of vertical model levels vs. level separation for the 90 level set and the 38 level set used in New Dynamics resolution tests.

Figure 6: 10m wind speed ($ms^{-1}$) at 13Z from 2kL38 forecast. The 10 $ms^{-1}$ wind contour is shown to indicate the extent of the low level Channel jet. The line, from (50.8°N, 0.2°W) to (49.7°N, 0.4°E), along which horizontal wind cross-sections were taken is also plotted.

closely match the "Old Dynamics" model levels, was used.

In addition to varying the horizontal grid resolution we also varied the vertical resolution of the model. We repeated the forecast run using the highest horizontal grid resolution of 2km, but increasing the number of vertical levels to 90 (run 2kL90). This 90 level set was generated using a stretched quadratic formula. Figure 5 shows a comparison of vertical height (without orography) vs. level separation for the two level sets.

Computational details for each of these runs are given in appendix A.

## 2.2 Verification

A variety of subjective verification measures were used for each model run. In line with the project aims, particular attention was paid to the low level winds. Isotach plots were produced on certain model levels. Note that for the models with 38 vertical levels, the lowest model level height is very close to 10m and we therefore use this for the 10m winds. The vertical structure of the winds was plotted as a cross-section taken across the English Channel, from (50.8°N, 0.2°W) to (49.7°N, 0.4°E), as shown in figure 6. Vertical wind profiles of the model winds were also examined at several points in the Channel along the Greenwich meridian; at Greenwich Light Vessel (50°25' N, 0°E) and at two points slightly further north, (50.5°N, 0°E) and (50.6°N, 0°E).

The thermal profiles and stability were also examined at these points. Cross-sections of theta were taken both from (51.35°N, 0.5°W) to (49.4°N, 0.5°W), (a section similar to that shown in figure 6 but including land points) and further upstream, across the entrance to the Dover Straits, from (51.3°N, 1.0°E) to (50.5°N, 2.0°E) and over the North Sea, from (52.1°N, 1.5°E) to (51.1°N, 2.5°E).

## 2.3 General Forecast Features

In each of the model runs a low-level jet develops in the English Channel. On a 10m wind plot this is clearly seen as a swathe of higher wind speeds extending from Dover westwards to the Isle of Wight and beyond. The jet shape is shown schematically in figure 6. It is clear that the extent of the jet is of the order of a hundred kilometres — it is not merely a headland effect. We note also that the jet is not symmetrical but rather runs along the northern half of the Channel, closer to the southern coast of England than to the French coast.

Examination of the vertical structure of the winds reveals that the jet maximum wind speed (of 16-17 $ms^{-1}$) actually occurs at a height of about 200m, but moves up to a height of approximately 300m and intensifies to 18-20 $ms^{-1}$ after 19Z.

The theta profiles and cross-sections taken over the Channel, show a mixed boundary layer close to the sea surface, capped by an inversion. The height and strength of this inversion vary both with location and during the course of the forecast day. In general the inversion is higher at 600-800m to the North over Kent and slopes downwards over the Channel, where the inversion height is 200-400m. The sloping nature of the inversion is caused by the isentropes descending and fanning out around the anticyclone. There may also be an element of boundary layer collapse over the sea.

During the day, strong mixing occurs over France and also over Sussex, lifting the boundary layer top there. In contrast, over Kent, the skies remained cloudy throughout the day, limiting the mixing in the boundary layer.

Further upstream, over the North Sea, the inversion is also sloping — from a height of 600-800m off the Suffolk coast to only 200-400m high off the Belgian coast. But,

from 16Z onwards, it becomes noticeably stronger and flatter - the height reduces to 300-400m just off the Suffolk coast, probably due to adiabatic descent. At the same time a corresponding descent of the inversion is evident over Kent, from a height of 800m to approximately 500m. With the inversion being so low, it is quite feasible that the Kent orography, which is 100-200m high, is having a blocking effect which contributes to the formation of the low-level jet in the Channel.

## 2.4 Comparison with the Operational "Old Dynamics" Mesoscale Forecast

The 12kL38 New Dynamics run (on the operational mesoscale domain) was compared with the operational UM 4.5 "Old Dynamics" mesoscale forecast from 0Z on 23/07/2000. In the "Old Dynamics" forecast a low-level Channel jet was also produced. However, as the forecast progresses, the 10m wind speeds are noticeably lower than in the New Dynamics Forecast; up to 1 $ms^{-1}$ slower from 06Z to 12Z and 2-3 $ms^{-1}$ slower later in the forecast as the jet spins up in the New Dynamics forecast. This is illustrated in figure 7, for 09Z and 21Z.

## 2.5 Impact of Horizontal Resolution

We now consider the differences between the forecast wind speeds from the New Dynamics model runs at varying horizontal resolution. The 10m wind speeds from the 2kL38, 4kL38 and 12kL38 forecast runs at 09Z and 13Z are shown in figure 8.

Firstly, we compared the model winds (on the lowest model level) with the observed 10m winds. The 2kL38 run verifies reasonably well up to T+7, during which period the winds observed at Greenwich LV are still below 25 knots. But from T+8 onwards, Greenwich LV regularly reports winds of 30 knots (although there is a slight slackening of the wind at 12Z). This maximum speed is not attained by any of the model forecasts.

For times up to 12Z, in the 4kL38 and 2kL38 forecasts, the maximum wind speeds in the eastern half of the Channel are notably larger ($\sim$ 0.5-1.5 $ms^{-1}$) than those attained in the 12kL38 run. It is, however, difficult to discern a distinct area of wind speed up above 10 $ms^{-1}$ (20 knots), except perhaps in the 2kL38 run.

From about 12Z onwards, a swathe of wind speeds of over 12 $ms^{-1}$ (ca. 24 knots) appears in each of the model forecasts at the eastern end of the English Channel between the south coast of England and Greenwich LV. The approximate shape of the jet at the 10m level is as indicated in figure 6, but note that the extent of the speed-up area increases with the model resolution. Thus the largest area of speed-up occurs for the 2kL38 run. The peak wind speed is also higher at 2km resolution, although the difference compared to the 12kL38 run is not as marked as in the earlier stages of the forecast. In addition, the region of wind speed-up 'hugs' the south coast of England more closely in the 4kL38 and 2kL38 runs, although this may be attributable to the higher resolution.

Differences between the model runs are also evident upon examination of the vertical structure of the jet. If we look at the wind profile from (50.6°N, 0°E), shown at 13Z in figure 9, 18km north of Greenwich Light Vessel, we see that the model winds from the lowest 300m of the atmosphere are consistently 1-2 $ms^{-1}$ greater in the 2kL38 and 4kL38 runs than in the 12kL38 run. The winds are also marginally faster in the highest resolution 2kL38 run, when compared to the 4kL38 run.

At Greenwich Light Vessel itself, (50°25' N, 0°E), the wind profiles from the three runs

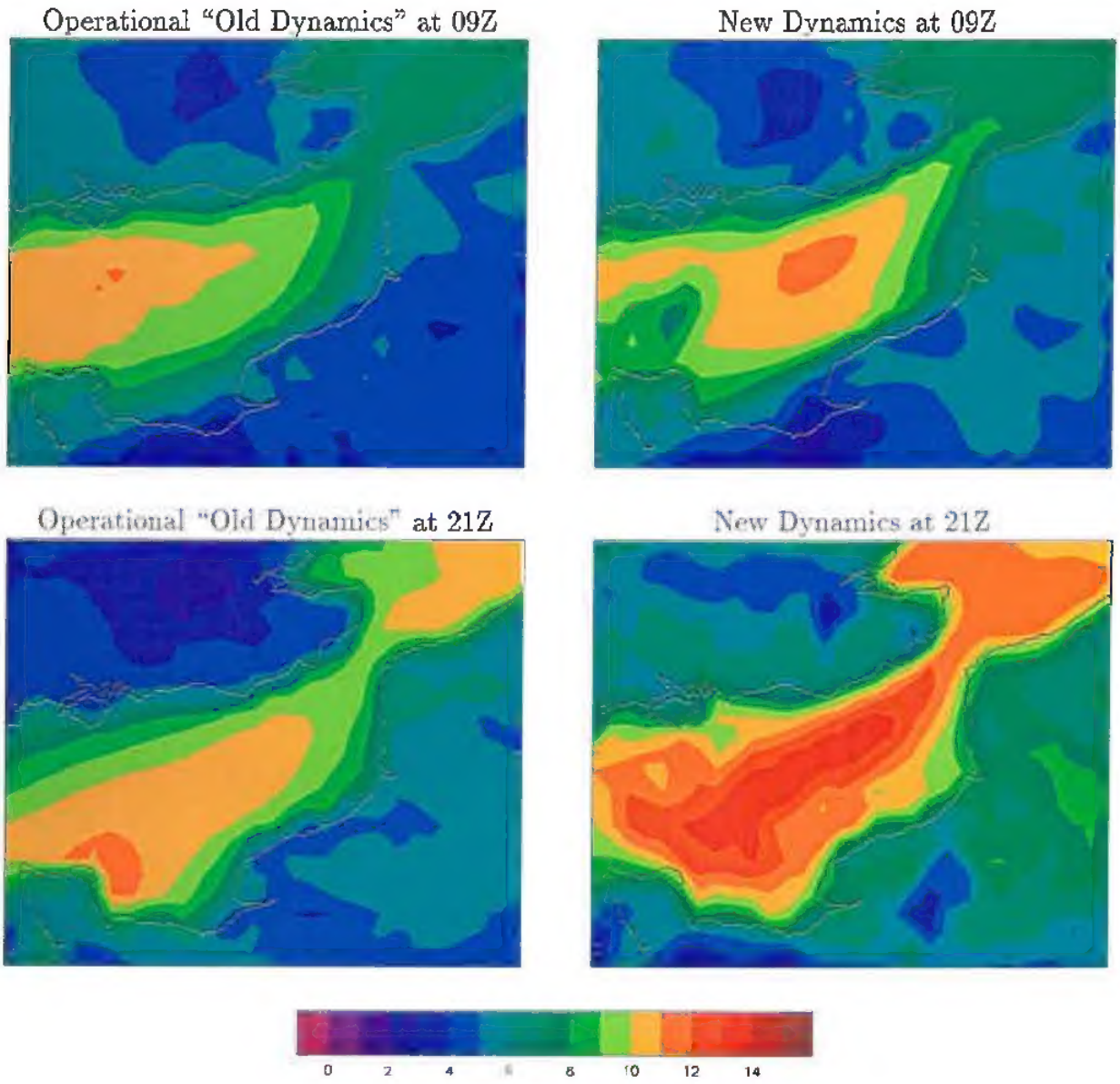


Figure 7: Comparison of 10m wind speeds (in $ms^{-1}$) over the Channel from the then operational UM 4.5 mesoscale forecast and the New Dynamics 12kL38 forecast at 09Z and 21Z.

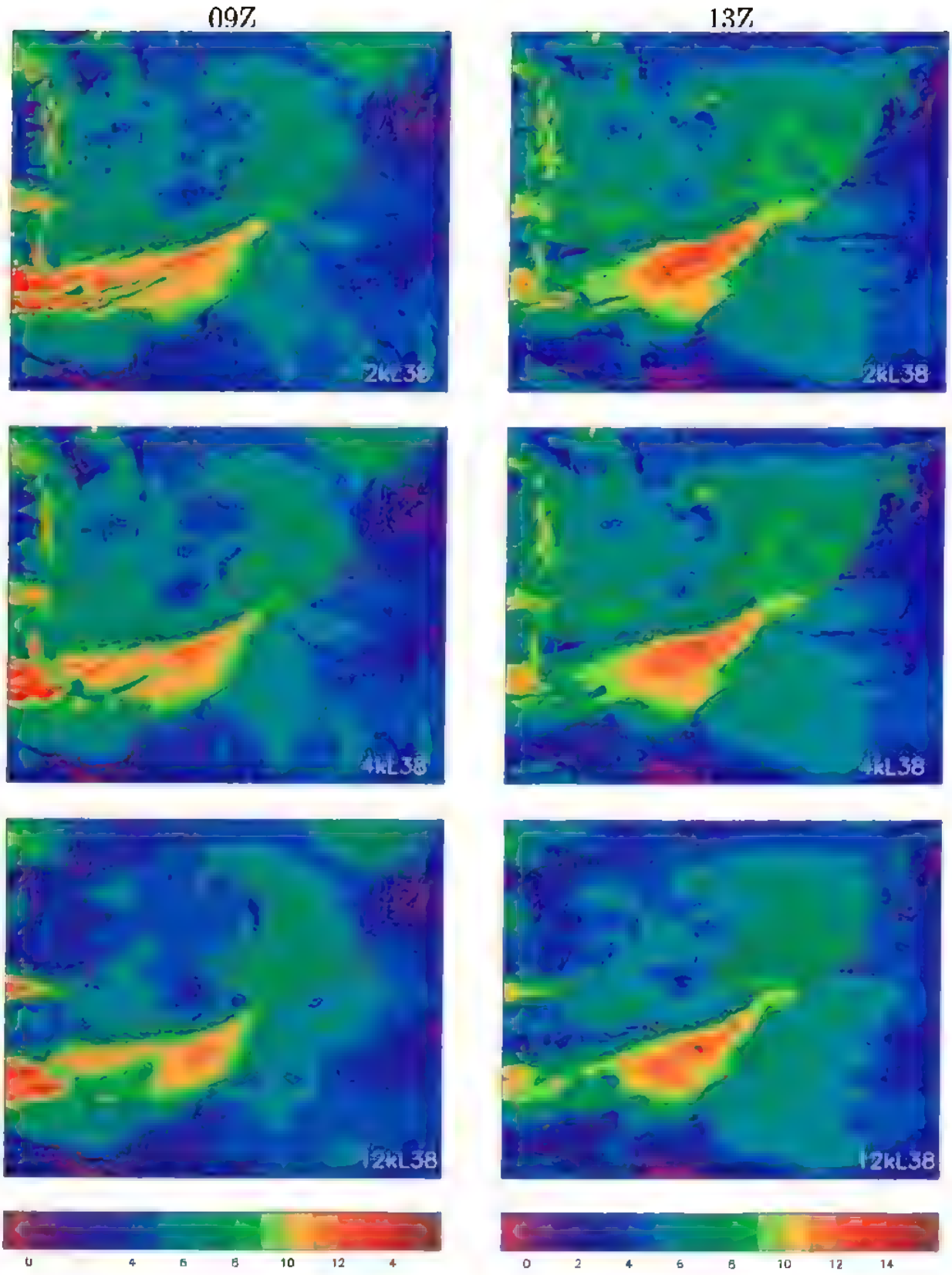


Figure 8: Forecast 10m wind speeds ($ms^{-1}$) at 09Z (left) and 13Z (right) from, from top to bottom, 2kL38, 4kL38 and 12kL38 models. All plots are shown on the 2km domain.

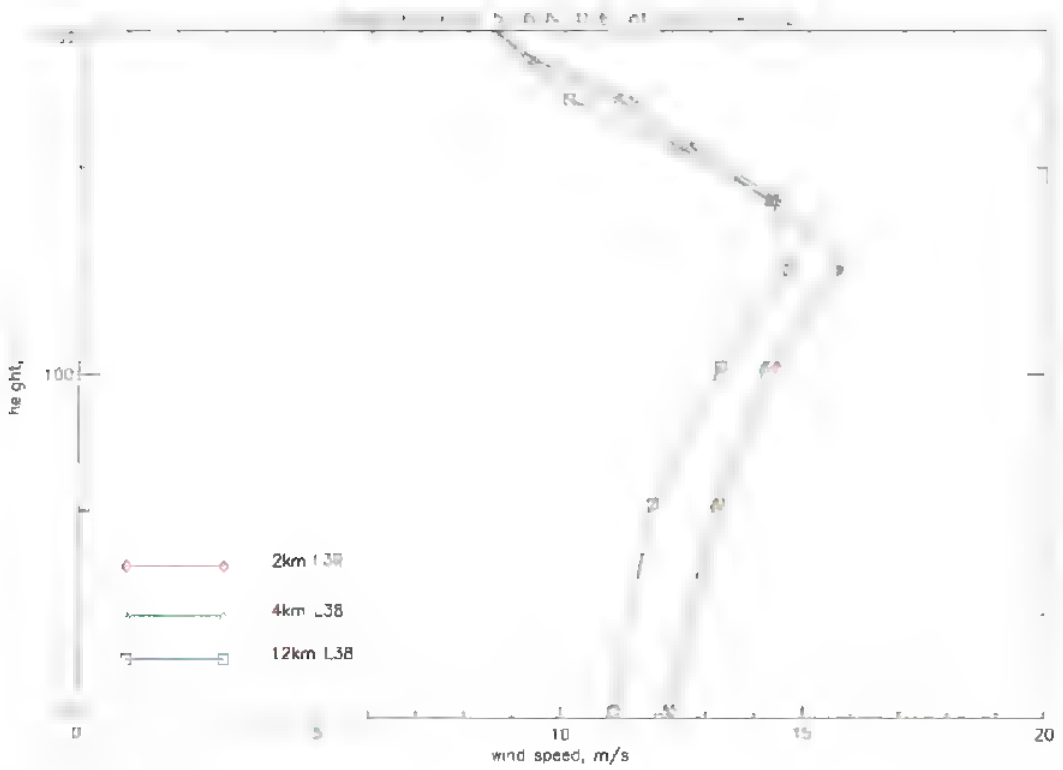


Figure 9: Wind Profile at 50.6°N, 0°E, at 13Z, for models at different horizontal resolution.

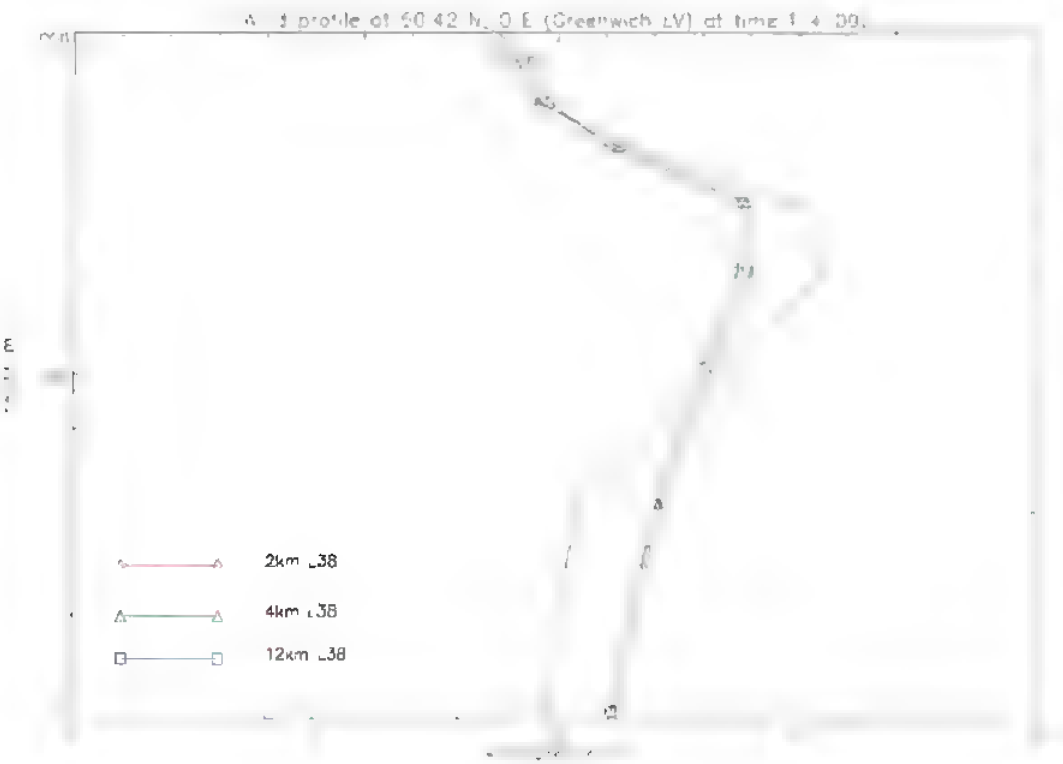


Figure 10: Wind Profile at Greenwich light vessel (50°25' N, 0°E), at 09Z, for models at different horizontal resolution.

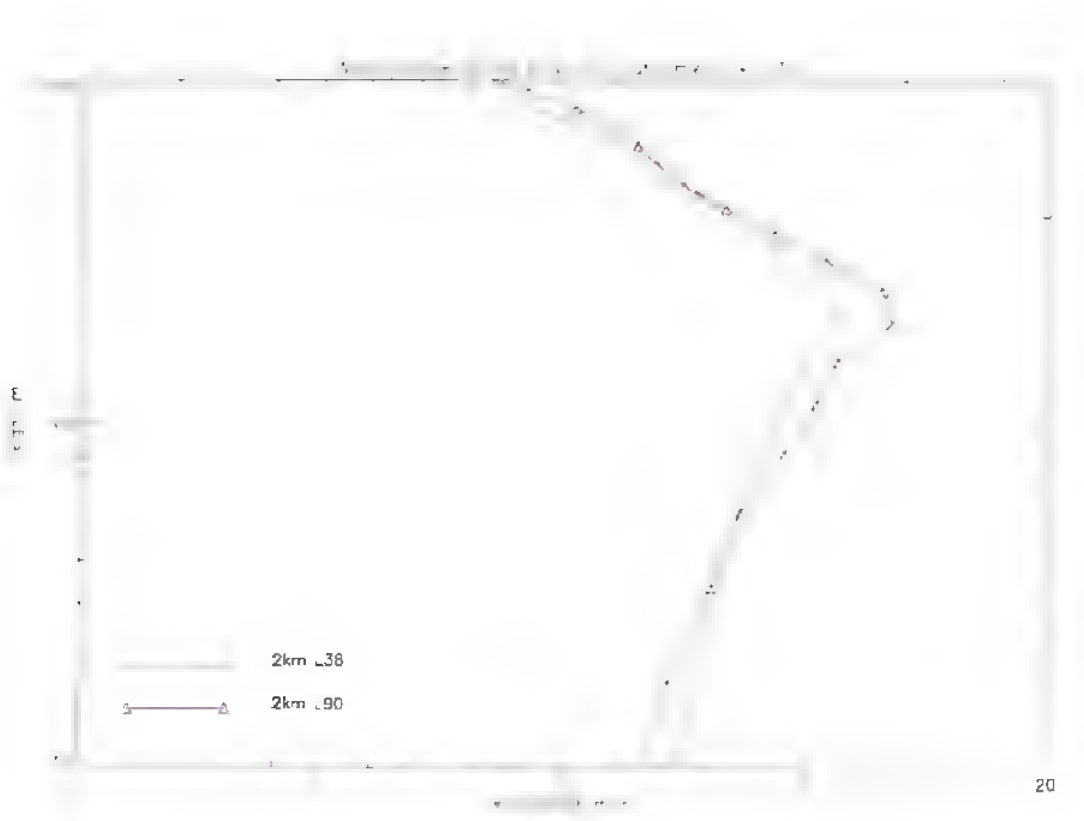


Figure 11: Wind Profile at 50.6°N, 0°E, at 13Z, for models at different vertical resolution.

are fairly similar, except at 9Z, shown in figure 10, where there is a pronounced difference in the 2kL38 run. It shows a jet maximum at 200m of 15.5 $ms^{-1}$, which is 2 $ms^{-1}$ greater than the maxima in the 12kL38 and 4kL38 runs. This is time at which a 10m wind speed of 30 knots was observed at Greenwich Light Vessel. As a caveat, we should note the danger of relying solely on one observation in the Channel for verification purposes. These winds are reported to first order within an accuracy of 5 knots and also the mast height of the Light Vessel is not totally reliable, winds are typically measured at 10-15m height.

Taken together, all these results indicate that the centre of the jet is actually slightly further north in the Channel than Greenwich light vessel, as this is where the highest wind speeds are seen.

## 2.6 Impact of Vertical Resolution

Now we consider the impact of increasing the number of vertical levels used from 38 to 90, whilst maintaining a horizontal grid spacing of 2km. Verification of the low-level winds was performed by the methods described above. The 10m wind speeds decreased overall in the 2kL90 run compared to the 38 level run. In addition, examination of vertical wind profiles in the Channel reveals that the winds close to the surface are up to 2 $ms^{-1}$ lower in the 90 level run. However if we look higher up, near the jet maximum at 200m height, both the vertical wind profiles and wind cross-sections show that, from 8Z onwards, the jet's maximum wind speed is about 1 $ms^{-1}$ faster in the higher vertical resolution, 90 level run. Figure 11 shows an example profile, taken at (50.6°N, 0°E), at 13Z.

In this case increasing the vertical resolution produces a faster jet maximum. The

spin up time is slightly shorter; the jet maximum is clearly visible in the vertical cross-section by 08Z (rather than 09Z in the 2kL38 case). The jet-trapping inversion is also better captured and is much sharper in the 2kL90 forecast. The magnitude of the vertical gradient, $\frac{\partial \theta}{\partial z}$ in the inversion region is approximately twice that in the 2kL38 forecast.

But why are the wind speeds close to the sea surface reduced and the wind shear in the low-level jet increased? The increased vertical resolution 2kL90 run could be more accurate, however the correlation with the observed 10m wind speeds is worse than in the 2kL38 case. Alternatively there may be a problem with the numerics of the model. In the 2kL90 run, the lowest model level is at 2m, as compared to 10m in the 2kL38 run. Thus, the numerical treatment of the surface stress and hence the vertical distribution of the stress will be different. It is possible that this is what is causing a local slowing of the wind over the sea surface. However the reduced 10m wind speeds could also be a non-local effect, due to incorrect calculation of the surface drag over land. Clearly this is a complex numerical and physical issue which requires further investigation.

# 3 Impact of Physical Parameters

## 3.1 Method

Having demonstrated the impact of resolution on the New Dynamics model forecast, we decided, as the next step in our investigation of the 23 July 2000 case, to probe the physical mechanism of the wind speed-up phenomenon. This was done by varying some of the physical parameters suspected of influencing the wind speed in the Dover Straits, specifically the surface roughness and the orography. These model runs were all performed using 2km horizontal grid spacing and 38 vertical levels, as in the 2kL38 run, which was taken as the reference run. The physical parameters were altered in each run as follows:-

1. Reference run ND 2kL38 (performed in Section 2)
2. Land surface roughness
   (a) decreased by factor of 100.0
   (b) increased by factor of 10.0
3. Sea surface roughness
   (a) decreased by factor of 10.0
4. Orography
   (a) removed
   (b) doubled
5. Reduced orography and land surface roughness, (i.e. 2a and 4a above combined)

In run 3a, the boundary layer code was altered, so that the sea surface roughness was multiplied by 0.1 immediately after being calculated according to the Charnock formula, for each timestep. Now, reducing the sea surface roughness leads to increased wind speed and hence increased surface friction velocity over the sea, which in turn leads to increased sea surface roughness. However, in practice, the roughness lengths produced by the model

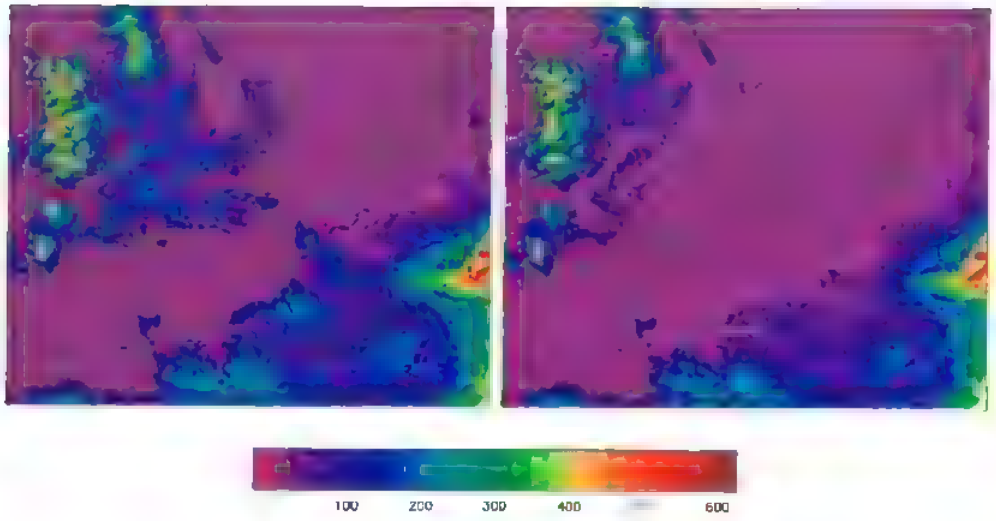


Figure 12: Left Orography for runs at 2km horizontal resolution (from DTED dataset). Right — Masked reduced orography used in runs 4a and 5.

over the sea in run 3a are indeed of the order of a tenth of those produced in the reference run 1, as desired.

For runs 4a and 5, the orography was reduced by means of a mask — as illustrated in figure 12 — which ensured that the orography was set to zero in the central portion of the domain but smoothed to the original orography at the boundaries. A similar mask was used to increase the orography for run 4b, again to avoid problems with the boundary conditions.

## 3.2 Results - Physical Experiments

In each of these experiments the model produces a low-level Channel jet, similar to that seen in the 2km L38 reference run 1. However the jet strength and intensity vary with the physical parameters. Differences are seen both in the maximum wind speed in the jet and in the contrast between the wind speeds over land and over the Channel.

As illustrated in figure 13, the maximum 10m wind speed in the Channel jet is influenced both by the orography and by the contrast in surface roughness as the wind flows from the sea over the land. Multiplying the surface roughness by a factor of 10.0 (run 2b) and doubling the orographic height (run 4b), both have a very similar effect on the magnitude of the maximum 10m wind speed, increasing it in the order of 1 $ms^{-1}$. Reducing the surface roughness length over the sea has an even more dramatic effect.

But, there is also great variation in the minimum wind speeds over land — and hence in the contrast between land and sea wind speeds — for the various model experiments. The forecast 10m wind speeds in the Channel at 13Z from each of the parameter experiments are plotted in figures 14 and 15. Figure 14 shows the impact of changing the orography and/or the land surface roughness length. Figure 15 compares the run with reduced sea surface roughness, 3a, to the reference run 1.

We now describe the results for each case in more detail.

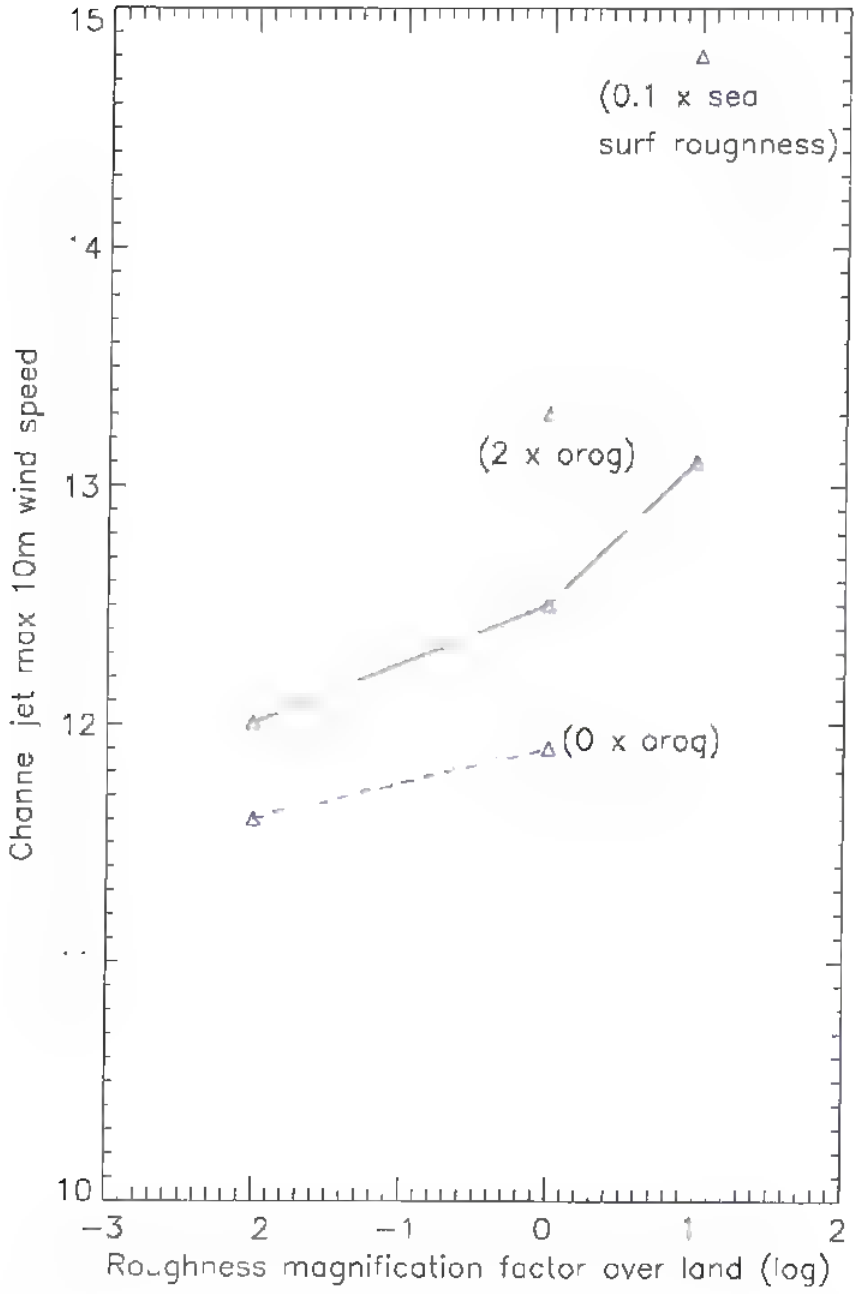


Figure 13: Maximum 10m wind speed in Channel jet vs. change in land surface roughness length for forecast at 13Z. Solid line joins runs with altered land surface roughness, 2a-1-2b. Runs with reduced orography, 4a and 5 are joined by a dotted line. Run 4b, with doubled orography is also shown. Reducing the sea surface roughness length in run 3a increases the land-to-sea roughness contrast by a factor of ten, hence its position on the graph.

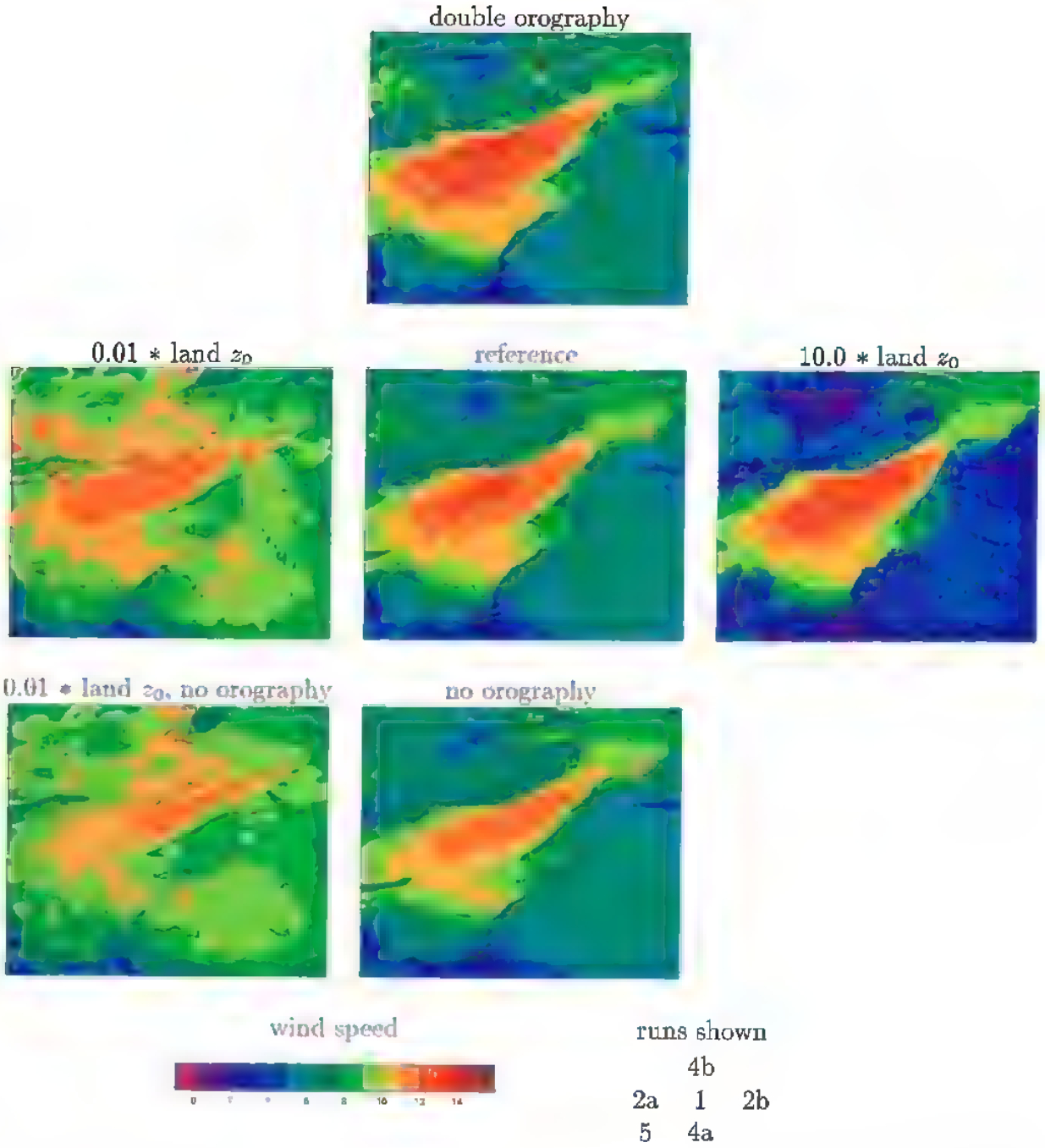


Figure 14: Forecast 10m wind speeds (in $ms^{-1}$) at 13Z from 0Z 23/07/2000 for physical parameter experiments, as land surface roughness is increased (left to right) and orography is increased (bottom to top). The reference run 1 is at the centre of the diagram, with the position of the other physical parameter experiment runs as indicated.

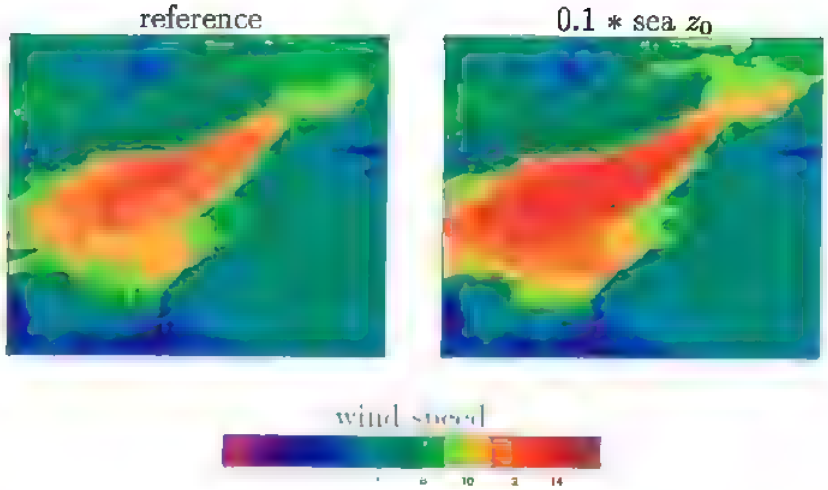


Figure 15: Forecast 10m wind speeds (in $ms^{-1}$) at 13Z from 0Z 23/07/2000 for reference run 1 and reduced sea surface roughness run 3a.

### 3.2.1 Orography

Increasing (4b) or decreasing (4a) the orography leads, as already noted, to a corresponding increase or decrease of order 1 $ms^{-1}$ in the maximum 10m wind speed. A change in wind speed of this magnitude is also seen throughout the depth of the Channel jet. Little difference is observed in the wind speeds over land specifically the Kent peninsula compared to the reference run 1, except that the winds are maybe slowed a little more (up to 1 $ms^{-1}$) over Kent when the orography is heightened.

### 3.2.2 Reduced Sea Surface Roughness

What happens when the surface roughness length is altered? Reducing the surface roughness length over the sea in run 3a leads, as expected, to an increase in wind speed over the Channel. However, this increase is not uniform throughout the jet. It is greatest close to the surface. At the 10m level, the wind speeds are of order 1.5 $ms^{-1}$ larger than in the reference run 1, with the difference increasing throughout the forecast to $\sim 2$ $ms^{-1}$ after 18Z. Also of note is that, from 12Z onwards, the 10m wind speeds are approximately 1 $ms^{-1}$ higher than in the runs 2b, in which the land surface roughness is increased and 4b, in which the orography is doubled.

At the height of the jet maximum, 200m, the wind speeds are also greater than in the reference run 1, but the increase in wind speed is up to 0.5 $ms^{-1}$ less than at the 10m level, close to the sea surface. The jet level wind speeds are also higher than in the reduced land surface roughness run 2b and the increased orography run 4b, but again the difference is not as great as at the 10m level.

The wind speeds over land are unaffected by the change in sea surface roughness and are similar to those in the reference run.

### 3.2.3 Land Surface Roughness

Increasing the surface roughness length over land (run 2b) causes an increase in wind speed in the Channel jet, compared to the reference run 1. Both at the 10m level and at the jet height the increase in the maximum wind speed is approximately 1 $ms^{-1}$.

Decreasing the surface roughness length over land (run 2a), leads to a similar decrease in the winds in the Channel jet.

Towards the end of the forecast period, the height of the jet is somewhat higher in the increased surface roughness case (2b), compared to the reference run (1), although this height difference is not more than 100m (or 1 model level).

We also need to consider the changes in the wind speed over land. Obviously, the wind will be slowed down as it impacts the land, which has a much higher surface roughness. In the reference run, the change in surface roughness as the wind impacts the Kent peninsula is $\sim 10^4$ and the maximum 10m wind speed in the jet is typically 6-7 $ms^{-1}$ greater than the lowest wind speeds produced by the model on land. When the land surface roughness is *reduced* by a factor of 100.0 in the model, (run 2a), there is only a $10^2$ sea to land increase in surface roughness as the wind impacts Kent. Along the Sussex coast the land surface roughness is roughly 10 times that over the sea. Consequently the difference between land and sea 10m wind speeds is halved to 3-4 $ms^{-1}$. Typical wind speeds over Kent in this run are much higher, (above 8-9 $ms^{-1}$) and therefore the contrast to the maximum Channel 10m wind speeds (which are lower than those in the reference run at 11-12 $ms^{-1}$) is considerably reduced. Conversely, when the land surface roughness is *increased* by a factor of 10.0, (run 2b), the maximum 10m jet speed increases but the wind speeds over land dramatically decrease - the minimum 10m wind speeds over Kent are of the order 2-4 $ms^{-1}$. The contrast between wind speeds over land and over sea is therefore 11-12 $ms^{-1}$, almost double that in the reference run.

### 3.2.4 Reduced Orography and Land Surface Roughness

Finally we consider model run 5, for which both the land surface roughness length and the orographic height were reduced. In this case, the 10m wind speeds over land were similar to those in run 2a, in which only the land surface roughness was reduced (by the same factor, 100.0). However the maximum wind speeds in the Channel, both at 10m and at jet height, were about 1 $ms^{-1}$ lower than in run 2a, indicating that both the surface roughness and the orography influence the formation and strength of the low level jet.

# 4 Conclusion

## 4.1 New Dynamics Forecast

For the 23 July 2002 case considered in this report, we have demonstrated, both from the observations and from the New Dynamics model forecasts, that wind speed-up in the Dover Straits and the English Channel did occur. A low-level Channel jet forms under a strong inversion. In the model forecasts this jet extends over a hundred kilometres along the south coast of England and hence cannot be perceived merely as a headland effect.

The New Dynamics forecast clearly contains much useful information. However, in this case, it takes some time for the model to spin up from the "Old Dynamics" analysis. This is not necessarily surprising if, as we suspect, Coriolis effects are important in the formation of the low-level jet. What is of note is that, once the New Dynamics model has spun up, we see a considerable improvement in terms of increased forecast wind speeds in the Channel jet even at the current operational mesoscale resolution compared to the "Old Dynamics"

## 4.2 Impact of Resolution on Forecast Quality

The maximum observed wind speed of 30 knots is not attained by any of the New Dynamics model forecasts of Section 2. Nevertheless, each of the forecasts shows a low-level Channel jet, the strength of which increases as the horizontal resolution implemented in the model increases. The forecast maximum wind speeds are greater, both at the 10m level and at 200m (where the jet is strongest), when the New Dynamics model is run at a horizontal grid resolution of 2km rather than 12km.

Increasing the vertical resolution, by using 90 rather than 38 model levels, also affects the forecast. At the 10m level the wind speeds are lower — possibly because the drag is being calculated incorrectly when the lowest model level is at a height of 2m. However, the low-level inversion, underneath which the jet is trapped, is stronger and better captured. At 200m height, where the jet is strongest, higher maximum wind speeds are predicted. Although the handling of the surface may need more attention, in general the forecast is improved when the vertical resolution is increased.

## 4.3 Physical Mechanisms

The numerical experiments performed in Section 3 demonstrate that the formation of the low-level Channel jet is influenced by both the sea-to-land surface roughness contrast and the surrounding orography. Increasing the height of the orography, increasing the land surface roughness or reducing the surface roughness over the sea all increase the speed of the Channel jet. However, the total impact on the forecast of each of these changes differs.

When the land surface roughness is increased, the wind speed increases in the Channel but also, obviously, the wind speeds over land decrease noticeably. In contrast, reducing the surface roughness of the sea, does not affect the wind speeds over land. But it does cause a differential alteration to the wind speeds over the sea; in the Channel jet the 10m wind speed is increased by a greater amount than the wind speed higher up in the jet at 200m.

We conclude that, in this case, the surface roughness change and the orography together lead to the low-level jet in the English Channel, as forecast by the model. In addition, it is obvious that the increased surface roughness over the Kent peninsula is the mechanism by which the wind speeds over land are decreased, providing definition to the low-level jet in the Channel. Hence a careful treatment of the surface roughness over land and sea and of the surface drag is clearly essential in order to guarantee accurate forecasts of the wind close to the sea surface, especially as the vertical resolution is increased.

## 4.4 Possible Strategies for Operational Implementation

In light of the overall long-term aim of the whole project — to improve the quality of low level atmospheric predictions — what has this case taught us about using the New Dynamics mesoscale model at high resolution as an operational forecast tool in such scenarios?

From our results, it is clear that as high a grid resolution as possible should be used, both in the horizontal and vertical directions This will bring direct improvement to the forecast, although obviously the grid size will be limited both by the available computer power and by the time constraints for producing a real time forecast.

A noticeable problem in the New Dynamics forecasts produced here is the time taken for the model to spin up the low level jet. How can a faster spin up of Coriolis effects be achieved?

We have already noted that the spin up is faster at a higher horizontal and vertical grid resolution. Also, the New Dynamics model forecast stronger winds in the Channel than the "Old Dynamics". We might therefore reasonably expect an improvement in the initial state, when the New Dynamics model is operational and we start a run from a New Dynamics analysis, rather than the "Old Dynamics" mesoscale analysis used here.

However, in the context of this project, a very high resolution — say 2km grid New Dynamics model forecast, is a product which may be required intermittently rather than being produced on a continuous operational basis. This raises a further question. Assume we have an operational forecast with or without data assimilation cycle at current mesoscale resolution, 12km, but we wish to run a very high resolution model at e.g. 2km grid resolution. What form, if any, of data assimilation should be used at this very high resolution and how would this reduce the spin-up time?

We briefly present some possible options.

### No Data Assimilation at High Resolution

The 12km New Dynamics analysis is used for the initial state. No information from smaller scales is included. This is clearly the cheapest strategy in terms of computational power, but means that the scales smaller than 12km, which proved to be very important in the case study considered here, will take time to spin up.

### Data Assimilation at High Resolution

An expensive computational strategy is to have full data assimilation at the very high 2km grid resolution as well as possibly at 12km resolution. This would retain the full detail of the jet in the initial model state. However there is always a risk that the assimilated observations may smooth out the jet, but this should not happen if it is well forecast.

### Nudging

A proposed middle way between the above two options is to separate the analysis field into a 12km resolution field and a field containing the very high resolution smaller scales, i.e. the difference of the 2km and 12km grid resolution fields. For the initial model state we would then use the 12km analysis and nudge in a very high resolution increment, calculated using linear analysis. With this approach there may be spin-up at the larger scales, above 12km, but it would be relatively small compared to the spin up required if no form of data assimilation were used.

Computationally, this strategy would be considerably cheaper than performing full data assimilation at 2km resolution, but we do not know at present if it is possible to implement in practice.

There is clearly considerable scope in choosing how to form the initial state. There are also trade-offs to be considered, for example, if no data assimilation is used at high resolution, then all the available computer power can be ploughed into increasing the grid resolution, but the spin-up time will be longer. Further trials are clearly necessary before the choice of data assimilation system for operational use can be finalised.

# 5 Proposals for Future Work

The case study described in this report has proved very informative, but one case study alone can neither prove the forecasting ability of the New Dynamics mesoscale model nor completely describe the wind speed-up phenomenon. Therefore, as the next stage in the project, we plan to consider further cases, either in the Dover Straits or in other coastal regions.

Several influencing factors could be quite different in another Dover Straits case, for example wind speed and direction, the stability profile of the atmosphere, the sea surface temperature or the surface temperature contrast. However, if our intention is to gain a better understanding of the phenomenon, we should aim to change only one or two of these variables in any one case.

We have already commented on the lack of observations which can be used for verification purposes, over the English Channel. One of our key aims would therefore be to perform a case study with more observational data. For this reason, we are considering how more data may be obtained, for example from sea traffic in the Channel or by using the new Met Office/NERC aircraft. We are also investigating whether higher density observational data is available in other coastal regions where similar wind speed-up phenomena occur. If so, these regions could be used for future modelling case studies.

In keeping with the broader aims of the Low Level Atmospheric Structure Project, the current and future cases will also be modelled using the 3dVOM model, a 3-dimensional time-dependent linear model developed at the University of Leeds. Comparison with the results from this model will be very valuable when deciding what forecasting tool is most practical for coastal regions while retaining the necessary degree of accuracy in its predictions.

# Acknowledgements

I would like to thank Eddy Carroll for suggesting the case studied here and Prof. Julian Hunt for providing the observational data from the Hoverspeed and for many useful and thought provoking discussions. Peter Clark was of great assistance at all stages of the project. Nigel Roberts and other colleagues at JCMM were also always willing to discuss and illuminate my findings.

# A New Dynamics Model Resolution Tests: Variable and Parameter Information

Tables 1 3 give more detailed information for each of the runs described in section 2. For further information see the New Dynamics Documentation [1] and the New Dynamics v3.0 User Guide [4].

## N.B.

1. Each run had a start time of 0Z 23/07/2000 and was run for 24 hours.
2. Each processor on T3EB has twice as much memory as those on T3EA. The T3EB processors are also a third faster, hence the timing for the 2kL38 and the 2kL90 runs cannot be directly compared.
3. The timings recorded are not necessarily reproducible. They should also be faster when the model is run in the UM rather than using the development version 3.0.

| Run | Grid $\Delta x, \Delta y$ (degrees) | Grid size (points) | Vertical levels | Timestep (mins) | Machine | NProc | Complete Code (seconds) | User CPU time (seconds) |
|---|---|---|---|---|---|---|---|---|
| 12kL38 | 0.11 | 146 x 182 | 38 | 5 | T3EA | 4 x 16 | n/a | n/a |
| 4kL38 | 0.04 | 250 x 250 | 38 | 2 | T3EA | 12 x 12 | 4 x $10^4$ | 2 x $10^6$ |
| 2kL38 | 0.02 | 340 x 280 | 38 | 1 | T3EA | 12 x 12 | 4 x $10^4$ | 6 x $10^6$ |
| 2kL90 | 0.02 | 340 x 280 | 90 | 1 | T3EB | 12 x 12 | 4 x $10^4$ | 4 x $10^6$ |

Table 1: Grid dimensions and computing resources.

| Run | Thermal Diffusion | | u,v-Wind Diffusion | | w-Wind Diffusion | |
|---|---|---|---|---|---|---|
| | order | coefficient | order | coefficient | order | coefficient |
| 12kL38 | 36*0,2*1 | 36*-1.0,2*1.7e+04 | 37*0,1 | 37*-1.0,1.7e+04 | 37*0 | 37*-1.0 |
| 4kL38 | 38*2 | 38*6.8e+03 | 38*2 | 38*6.8e+03 | 37*2 | 37*6.8e+03 |
| 2kL38 | 38*2 | 38*3158.0 | 38*2 | 38*3158.0 | 37*2 | 37*3158.0 |
| 2kL90 | 88*-1,2*1 | 88*0.0e+04,2*1.4e+03 | 89* 1,1 | 89*0.0e+04,1.4e+03 | 89*0 | 89*-1.0 |

Table 2: Diffusion namelist entries.

| Run | Implicit Weights | | | | GCR-tol | | iterations |
|---|---|---|---|---|---|---|---|
| | $\alpha_1$ | $\alpha_2$ | $\alpha_3$ | $\alpha_4$ | | | |
| 12kL38 | 0.6 | 1.0 | 0.6 | 1.0 | abs | 5.e-3 | n/a |
| 4kL38 | 0.7 | 1.0 | 0.7 | 1.0 | abs | 5.e-4 | 20-30 |
| 2kL38 | 0.7 | 1.0 | 0.7 | 1.0 | abs | 1.e-5 | 65 66 |
| 2kL90 | 0.7 | 1.0 | 0.7 | 1.0 | abs | 1.e-5 | 72-77 |

Table 3: Weights and gcrparams namelist entries and approximate number of iterations required by GCR solver.

# References

[1] Staniforth, A. et al, 2001: The Joy of UM 5.2 - Model Formulation, Unified Model Documentation Paper No 15, Crown Copyright - unpublished

[2] Baines, P.G., 1979: Observations of Stratified Flow Past Three-Dimensional Barriers, J. Geophys. Research, **84**, 7834-7838

[3] Baines, P.G., 1995: Topographic Effects in Stratified Flows, CUP

[4] Malcolm, A.J., Gardner, Z.E. and Mawson, M.H., 2000: User Guide to Running the Proposed Semi-Implicit Integration Scheme for the Unified Model, Version 3.0, in 3D Mode, unpublished

## CURRENT JCMM INTERNAL REPORTS

This series of JCMM Internal Reports, initiated in 1993, contains unpublished reports and also versions of articles submitted for publication. The complete set of Internal Reports is available from the National Meteorological Library on loan, if required.

1. **Research strategy and programme**
   K A Browning et al
   January 1993

2. **The GEWEX Cloud System Study (GCSS)**
   **GEWEX Cloud System Science Team**
   January 1993

3. **Evolution of a mesoscale upper tropospheric vorticity maximum and comma cloud from a cloud-free two dimensional potential vorticity anomaly**
   K A Browning
   January 1993

4. **The global energy and water cycle**
   K A Browning
   July 1993

5. **Structure of a midlatitude cyclone before occlusion**
   K A Browning and N Roberts
   July 1993

6. **Developments in systems and tools for weather forecasting**
   K A Browning and G Szejwach
   July 1993

7. **Diagnostic study of a narrow cold frontal rainband and severe winds associated with a stratospheric intrusion**
   K A Browning and R Reynolds
   August 1993

8. **Survey of perceived priority issues in the parametrizations of cloud-related processes in GCMs**
   K A Browning
   September 1993

9. **The effect of rain on longwave radiation**
   I Dharssi
   September 1993

10. **Cloud microphysical processes - a description of the parametrization used in the large eddy model**
    H Swann
    October 1993

11. **An appreciation of the meteorological research of Ernst Kleinschmidt**
    A J Thorpe
    May 1992

12. **Potential vorticity of flow along the Alps**
    A J Thorpe, H Volkert and Dietrich Heimann
    August 1992

13. **The representation of fronts**
    A J Thorpe
    January 1993

14. **A parametrization scheme for symmetric instability: test for an idealised flow**
C S Chan and A J Thorpe
February 1993

15. **The Fronts 92 Experiment: a Quicklook Atlas**
Edited by T D Hewson
November 1993

16. **Frontal wave stability during moist deformation frontogenesis**
**Part 1: Linear wave dynamics**
C H Bishop and A J Thorpe
May 1993

17. **Frontal wave stability during moist deformation frontogenesis**
**Part 2. The suppression of non-linear wave development**
C H Bishop and A J Thorpe
May 1993

18. **Gravity waves in sheared ducts**
S Monserrat and A J Thorpe
October 1993

19. **Potential vorticity and the electrostatics analogy: quasi-geostrophic theory**
C Bishop and A J Thorpe
November 1993

20. **Recent advances in the measurement of precipitation by radar**
A J Illingworth
April 1993

21. **Micro-physique et givrage: cloud microphysics and aircraft icing**
A J Illingworth
May 1993

22. **Differential phase measurements of precipitation**
M Blackman and A J Illingworth
May 1993

23. **Estimation of effective radius of cloud particles from the radar reflectivity**
N I Fox and A J Illingworth
May 1993

24. **A simple method of Dopplerising a pulsed magnetron radar**
A Hua, A J Illingworth and J Eastment
November 1993

25. **Radiation and polar lows**
George C Craig
February 1994

26. **Collected preprints submitted to the International Symposium on the Life Cycles of Extratropical Cyclones; Bergen, Norway, 27 June - 1 July 1994**
April 1994

27. **Convective frontogenesis**
Douglas J Parker and Alan J Thorpe
April 1994

28. **Improved measurement of the ice water content in cirrus using a total water evaporator**
Philip R A Brown and Peter N Francis
April 1994

29. **Mesoscale effects of a dry intrusion within a vigorous cyclone**
K A Browning and B W Golding
April 1994

30. **GEWEX Cloud System Study, Science Plan**
May 1994

31. **Parametrization of momentum transport by convectively generated gravity waves**
R Kershaw
May 1994

32. **Mesoscale Modelling Newsletter No 5**
May 1994

33. **Observations of the mesoscale sub-structure in the cold air of a developing frontal cyclone**
K A Browning, S A Clough, C S A Davitt, N M Roberts and T D Hewson
May 1994

34. **Longwave radiative forcing of a simulated tropical squall line**
Imtiaz Dharssi
July 1994

35. **On the nature of the convective circulation at a kata-cold front**
K A Browning
September 1994

36. **Collective preprints of papers submitted to the COST-75 International Seminar on Advanced Weather Radar Systems, Brussels, 20-23 September 1994**
November 1994

37. **Use of satellite imagery to diagnose events leading to frontal thunderstorms: Parts I and II of a case study**
K A Browning and N M Roberts
November 1994

38. **The role of spaceborne millimetre-wave radar in the global monitoring of ice cloud**
P R A Brown, A J Illingworth, A J Heymsfield, G M McFarquhar, K A Browning and M Gosset
December 1994

39. **Potential vorticity inversion**
Michal Ziemianski
October 1994

40. **Theory of mature tropical cyclones; a comparison between Kleinschmidt (1951) and Emanuel (1986)**
Suzanne L Gray
December 1994

41. **Dispersion and removal of pollutants during the passage of an atmospheric frontal system**
N R Gimson
December 1994

42. **The role of snow sublimation in frontogenesis**
D J Parker and A J Thorpe
December 1994

43. **Potential vorticity and the electrostatics Analogy: Ertel-Rossby formulation**
A J Thorpe and C H Bishop
December 1994

44. **Mesoscale aspect of extratropical cyclones: an observational perspective**
K A Browning
January 1995

45. **A polar low outbreak: evolution and mesoscale structures**
T D Hewson, G C Craig and C Claud
February 1995

46. **Generation of near-surface gusts of deep convection**
K Nakamura and R Kershaw
April 1995

47. **Attribution concepts applied to the Omega Equation**
S A Clough, C S A Davitt and A J Thorpe
June 1995

48. **Parametrization of mixed-phase cloud and precipitation**
Susan P Ballard and M Gerard Hutchinson
June 1995

49. **Short-range forecasting of stratocumulus: initialization prediction**
Susan P Ballard, Simon D Jackson and B Macpherson
June 1995

50. **Contributions of the JCMM/Dept of Meteorology Radar Group to the 27th AMS Radar Meteorology Conference, Vail October 1995**
June 1995

51. **Cold pools in shear**
Douglas J Parker
September 1995

52. **High-resolution analysis of frontal fracture**
K A Browning, S P Ballard and C S A Davitt
September 1995

53. **The albedo of broken cloud fields: calculations using a modified two stream radiation code**
Imtiaz Dharssi and Roy Kershaw
October 1995

54. **Parametrization of momentum transport by convection. I: theory and cloud modelling results**
R Kershaw and D Gregory
November 1995

55. **Variation of frontal structure along a cold front**
K A Browning and N M Roberts
November 1995

56. **Secondary frontal waves**
Douglas Parker
December 1995

57. **Objective fronts**
T D Hewson
March 1996

58. **Mesoscale analysis of the activation of a cold front during cyclogenesis**
K A Browning, N M Roberts and A J Illingworth
June 1996

59. **Investigation of different representations of rain in a 1-d evaporation model**
H Swann
May 1996

60. **Parametrization of diabatic processes in the inversion of the omega-equation**
M Athanassiadou and A J Thorpe
June 1996

61. **The role of the environmental flow in the development of secondary frontal cyclones**
I A Renfrew, A J Thorpe and A Joly
June 1996

62. **Consequences of the geostrophic momentum approximation on barotropic instability**
S Malardel, A J Thorpe and A Joly
June 1996

63. **Contributions to the AMS/RMS Conference on Mesoscale Processes**
Reading, 9-13 September 1996

64. **Vorticity and potential vorticity in stratified flows interacting with an isolated obstacle**
Jorge A Gutiérrez and A J Thorpe
September 1996

65. **Triple point development: two case studies**
Douglas Parker
September 1996

66. **Radar observations of wind-shear splitting within evolving atmospheric Kelvin-Helmholtz billows**
D Chapman and K A Browning
April 1997

67. **Cold frontal structure derived from radar wind profilers**
K A Browning, D Jerrett, J Nash, T Oakley and N M Roberts
May 1997

68. **The dry intrusion and its effect on the frontal, cloud and precipitation structure of extratropical cyclones**
K A Browning - Text of invited special lecture at the Spring Conference
of the Meteorological Society of Japan, University of Tsukuba, 22 May 1997

69. **Met. Office Unified Model data, diagnostics, graphics programs, and other observational data available from the JCMM through the aegis of the Universities Weather Research Network (UWERN).** (Plus supplement)
Peter Panagi and Ed Dicks
June 1997

70. **Contributions of the JCMM/Dept of Meteorology Radar Group to the 28th AMS Radar Meteorology Conference.** Austin, Texas
September 1997

71. **Sensitivity of short-range weather forecasts to local potential vorticity modifications**
Meral Demirtas and Alan Thorpe
July 1997

72. **Objective identification of frontal wave cyclones**
T D Hewson
August 1997

73. **Attribution and its application to mesoscale structure associated with tropopause folds**
A J Thorpe
September 1997

74. **The role of the environmental flow in the development of secondary frontal cyclones**
Ian A Renfrew, Alan J Thorpe and Craig H Bishop
September 1997

75. **Potential vorticity: a short history of its definitions and uses**
Alan J Thorpe and Hans Volkert
September 1997

76. **Superposing semi-geostrophic potential vorticity anomalies**
H R Birkett and A J Thorpe
September 1997

77. **Short period forecasting of catchment-scale precipitation.**
**Part 1: the role of Numerical Weather Prediction**
M A Pedder, M Haile and A J Thorpe
September 1997

78. **Verification of the tracking technique used in an experimental cloud motion wind inferring system**
Z Wang, K A Browning and G A Kelly
October 1997

79. **A preliminary study of Fourier series analysis for cloud tracking with GOES high temporal resolution images**
Z Wang
October 1997

80. **Analysis of an ex-tropical cyclone after reintensifying as a warm-core extratropical cyclone**
K A Browning, G Vaughan and P Panagi
November 1997

81. **A JCMM overview of FASTEX IOPs**
S A Clough, H W Lean, N M Roberts, H Birkett, J-P Chaboureau, R Dixon, M Griffiths, T D Hewson and A Montani
January 1998

82. **Programs for PV inversion and modification**
Meral Demirtas
December 1997

83. **Release of potential shearing instability in warm frontal zones**
D Chapman and K A Browning
February 1998

84. **The European Cloud-Resolving Modelling Programme ( EUCREM)**
Summary Report from the coordinator
P W White
April 1998

85. **A frontal wave database**
T D Hewson
April 1998

86. **Layering observed in dropsoundings from IOP 1 of Fronts 92**
S A Clough
May 1998

87. **Use of wind-shear displays for Doppler radar data**
D Chapman and K A Browning
May 1998

88. **Radar estimates of rainfall rates at the ground in bright band and non-bright band events**
T J Smyth and A J Illingworth
June 1998

89. **Correction for attenuation of radar reflectivity using polarisation data**
T J Smyth and A J Illingworth
June 1998

90. **The effects of convection on chemical reactions and precipitation scavenging**
Neil R Gimson
July 1998

91. **How to use the display program DISP**
Nigel Roberts
August 1998

92. **Conceptual models of cyclogenesis**
Adrian T Semple
August 1998

93. **Observations of oblate hail using dual polarisation radar and implications for hail detection schemes**
T J Smyth, T M Blackman and A J Illingworth
September 1998

94. **The semigeostrophic diagnosis of vertical motion. Part I: Formulation and co-ordinate transformations**
Mike A Pedder and Alan J Thorpe
September 1998

95. **The semigeostrophic diagnosis of vertical motion. Part II: Results for an idealised baroclinic wave life cycle**
Alan J Thorpe and Mike A Pedder
September 1998

96. **Convective destabilisation by a tropopause fold diagnosed using potential vorticity inversion**
Morwenna Griffiths, Alan Thorpe and Keith Browning
October 1998

97. **Forecast skill of the ECMWF model using targeted observations during FASTEX**
A Montani, A J Thorpe, R Buizza and P Unden
October 1998

98. **Observations and model simulations of the FASTEX IOP 16 frontal wave - effects of sublimation**
Sid A Clough, Humphrey W Lean, Nigel M Roberts and Richard M Forbes
December 1998

99. **The application of conceptual models in NWP**
Adrian T Semple
January 1999

100. **Mesoscale analysis of arc rainbands in a dry slot**
K A Browning and N M Roberts
January 1999

101. **Interaction of mesoscale tropopause depressions with a warm-core cyclone: observational and model analyses, and sensitivity to analysis errors**
K A Browning, A J Thorpe, A Montani, D Parsons, M Griffiths, P Panagi and E M Dicks
February 1999

102. **The use of water vapour imagery and PV inversion to adjust initial conditions in NWP**
Sean J Swarbrick
February 1999
*This report is no longer available; see Internal Report No.108*

103. **Summary notes for a lecture course on Waves in the Atmosphere and Ocean**
A A White
March 1999

104. **Results of a questionnaire on the operational value of conceptual models (CMs) of fronts and cyclones**
N M Roberts & M V Young
July 1999

105. **Contributions to the Poster Session at the 1998 UWERN Annual Science Meeting**
assembled by A A White
August 1999

106. **The objective analysis of dropsonde data from FASTEX**
Richard Forbes, Sid Clough, Mark Dixon, Andy Macallan & Nigel Roberts
January 2000

107. *NWP Technical Report No.302*
**Implications for Mesoscale Modelling from a Study of the FASTEX IOP 16 Mid-latitude Cyclone**
Richard M Forbes, Humphrey W Lean, Nigel M Roberts and Peter A Clark
March 2000

108. *NWP Technical Report No.291*
**The use of water vapour imagery and PV inversion to adjust initial conditions in NWP**
Final Project Report
Sean J Swarbrick
September 1999

109. *NWP Technical Report No.294*
**A guide to aspects of water vapour imagery interpretation: the significance of dry regions**
Nigel M Roberts
January 2000

110. *NWP Technical Report No.300*
**The relationship between water vapour imagery and thunderstorms**
Nigel M Roberts
February 2000

111. *NWP Technical Report No.293*
**Holomorphic structures in hydrodynamical models of nearly geostrophic flow**
V N Roubtsov and I Roulstone
January 2000

112. *NWP Technical Report No.301*
**Multi-sensor synthesis of the mesoscale structure of a cold-air comma cloud system**
K A Browning, P Panagi and E M Dicks
March 2000

113. *NWP Technical Report No.307*
**Observations of stratospheric air entering the circulation of a polar low**
K A Browning and E M Dicks
May 2000

114. *NWP Technical Report No.309*
**Wind profiler – Unified Model comparison statistics**
Peter Panagi & Ed Dicks
March 2000

115. *NWP Technical Report No.310*
**Towards a similarity theory of moist convective updrafts**
Olaf Stiller and George C Craig
May 2000

116. *NWP Technical Report No.312*
**The mystery of striated cloud heads in satellite imagery**
R S Dixon, K A Browning and G J Shutts
April 2000

117. *NWP Technical Report No.313*
**MDIAG: a Fortran 90 program to compute diagnostics on pressure levels from Unified Model data on model levels**
Peter Panagi
June 2000

118. *NWP Scientific Paper No.56*
**Rearrangements of functions with applications to meteorology and ideal fluid flow**
R J Douglas
June 2000

119. *NWP Technical Report No.320*
**Tests of New Dynamics Model on the FASTEX IOP16 case**
Humphrey Lean
September 2000

120. *NWP Scientific Paper 57*
**A classification of FASTEX cyclones using a height-attributable QG vertical motion diagnostic**
A C L Deveson, K A Browning, T D Hewson
September 2000

121. *NWP Scientific Paper 59*
**Measurements of dissipation rate in frontal zones**
D.Chapman, K A Browning
August 2000

122. *NWP Technical Report 331*
Not Issued

123. *NWP Technical Report 337*
**A Case Study of High Resolution Fog Forecasts with the New Dynamics**
P. Clark
November 2000

124. *NWP Technical Report 338*
**Comparison of ECMWF Winter-Season Cloud Fraction with Radar Derived Values**
Robin J. Hogan, Christian Jakob, Anthony J. Illingworth
January 2001

125. *NWP Technical Report 339*
**Deriving Cloud overlap statistics from radar**
Robin J. Hogan, Anthony J. Illingworth
January 2001

126. *NWP Technical Report 344*
**Results from simulations of an organised convective event using the New Dynamics at 12, 4 and 2km resolution.**
Nigel Roberts
January 2001

127 *NWP Technical Report 348*
**A North Atlantic Survey of Cyclogenesis in 1999: Unified Model Performance in Short Range Forecasts & The Relationship Between Potential Vorticity, Water Vapour Imagery and Analysis Accuracy.**
Adrian Semple
March 2001

128 NWP Scientific Paper 61
Are there higher-accuracy analogues of semigeostrophic theory?
Ian Roulstone, Michael E. McIntyre
June 2001

129 NWP Scientific Paper 62
Stacked slantwise convective circulations
K A Browning, D Chapman, R S Dixon
April 2001

130 NWP Technical Report 357
A Meteorological Assessment of the Geostrophic Co-ordinate Transform and Error Breeding System when used in 3D Variational Data Assimilation.
Adrian Semple
June 2001

131 NWP Scientific Paper 63
The dynamics of a mid-latitude cyclone with very strong latent heat release
Farhang Ahmadi-Givi, George Craig
July 2001

132 NWP Scientific Paper 64
A Study of the Effects of Horizontal and Vertical Resolution in the New Dynamics representation of FASTEX IOP16
Humphrey Lean
October 2001

133 NWP Scientific Paper 66
Modelling Low Level Winds with the Met Office New Dynamics Model
Rachel Anne Capon
9 May 2002

**Met Office** Joint Centre for Mesoscale Meteorology Department of Meteorology
University of Reading PO Box 243 Reading RG6 6BB United Kingdom
Tel: +44 (0)118 931 8425 Fax: +44 (0)118 931 8791
www.metoffice.com